

Measuring proximity to standard planes during fetal brain ultrasound scanning*

Chiara Di Vece^{1,2}, Antonio Cirigliano¹, Meala Le Lous^{1,3,4}, Raffaele Napolitano^{5,6}, Anna L. David^{1,7}, Donald Peebles^{1,7}, Pierre Jannin⁴, Francisco Vasconcelos^{1,2}, and Danaïl Stoyanov^{1,2}

¹ Wellcome/EPSRC center for Interventional and Surgical Sciences (WEISS),
University College London (UCL), London, UK

² Dept of Computer Science, UCL, London, UK

³ Dept of Obstetrics and Gynecology, University Hospital of Rennes, Rennes, France

⁴ Univ Rennes, INSERM, LTSI - UMR 1099, F35000, Rennes, France

⁵ Fetal Medicine Unit, Elizabeth Garrett Anderson Wing, UCLH NHS Foundation Trust, London, UK

⁶ Elizabeth Garrett Anderson Institute for Women's Health, UCL, London, UK

⁷ Dept of Obstetrics and Gynecology, UCLH, London, UK

chiara.divece.20@ucl.ac.uk

Abstract. This paper introduces a novel pipeline designed to bring ultrasound (US) plane pose estimation closer to clinical use for more effective navigation to the standard planes (SPs) in the fetal brain. We propose a semi-supervised segmentation model utilizing both labeled SPs and unlabeled 3D US volume slices. Our model enables reliable segmentation across a diverse set of fetal brain images. Furthermore, the model incorporates a classification mechanism to identify the fetal brain precisely. Our model not only filters out frames lacking the brain but also generates masks for those containing it, enhancing the relevance of plane pose regression in clinical settings. We focus on fetal brain navigation from two-dimensional (2D) ultrasound (US) video analysis and combine this model with a US plane pose regression network to provide sensorless proximity detection to SPs and non-SPs planes; we emphasize the importance of proximity detection to SPs for guiding sonographers, offering a substantial advantage over traditional methods by allowing earlier and more precise adjustments during scanning. We demonstrate the practical applicability of our approach through validation on real fetal scan videos obtained from sonographers of varying expertise levels. Our findings demonstrate the potential of our approach to complement existing fetal US technologies and advance prenatal diagnostic practices.

Keywords: Ultrasound · Fetal brain · Semantic segmentation · Semi-supervised learning.

* This work was supported in whole, or in part, by the Wellcome/EPSRC Centre for Interventional and Surgical Sciences (WEISS) [203145/Z/16/Z], the Department of Science, Innovation and Technology (DSIT) and the Royal Academy of Engineering under the Chair in Emerging Technologies programme.

1 Introduction

Fetal US is instrumental in the early detection of fetal growth abnormalities, potentially averting adverse outcomes for both mother and child [1]. The efficacy of US screenings largely hinges on the operator’s skill in navigating to and reproducing standard imaging planes, known as SPs, which demands spatial awareness, precise hand-eye coordination, and thorough anatomical knowledge. Novices often find the requisite multitasking overwhelming, struggling to manipulate the transducer while interpreting the 2D images as representations of three-dimensional (3D) structures [2,3]. Furthermore, the variability in examination outcomes due to differing levels of operator experience can cause measurement and diagnostic discrepancies, challenging the reliability of fetal US diagnostics [4]. International guidelines underscore the critical role of US in diagnosing fetal growth disorders, highlighting the need for standardized scanning protocols and quality control measures [5].

Artificial intelligence (AI) offers promising solutions to address these challenges in different ways. Images of the various SPs can be reliably recognized in real-time with classifier networks [6], and standardized biometry measurements on those planes can also be automated [7,8,9]. Based on these image recognition capabilities, the freehand US scanning process can be simplified to reduce inter-operator variability by automatically extracting SPs from 3D US volumes [10,11]. Most of these techniques assume that a good quality US scan has already been acquired in the correct position and only assist in image analysis.

A range of other approaches aims at providing spatial localization of the US acquisition plane so that less experienced sonographers can more effectively navigate to SPs. Some rely on additional sensors attached to the US probe [12,13], while others are purely image-based [14,15,16], leveraging 3D US brain volumes as training data. The latter methods are attractive as they can potentially be deployed on conventional 2D US probes typically used in clinical practice, but they still face some challenges in translation. They have only been substantially validated on slices of 3D US volumes, which is still not the final intended usage. Bringing them closer to translation, Yeung et al. [17] have fine-tuned their model on 2D US video in a self-supervised way. Additionally, while these methods output a six-dimensional (6D) pose of a US plane, it is still poorly understood how to communicate this information to a sonographer for effective navigation.

This paper proposes a pipeline that aims at bringing US plane pose estimation closer to a practical use case of assisted navigation, focusing on fetal brain navigation from 2D US video analysis. Our envisaged system (Figure 1) detects when the fetal brain is being visualized and provides a proximity signal to a specific target SP (we consider transventricular (TV) SP in this work). The contributions can be summarised as follows: 1) We propose a fetal brain segmentation and classification model (SS-Seg+Class) that works reliably for arbitrary sections of the brain. We achieve this in a semi-supervised manner, using a set of labeled SP images together with unlabeled slices from 3D US volumes; 2) We combine this segmentation model with a US plane pose estimation network, improving accuracy with respect to an end-to-end baseline; 3) We manually an-

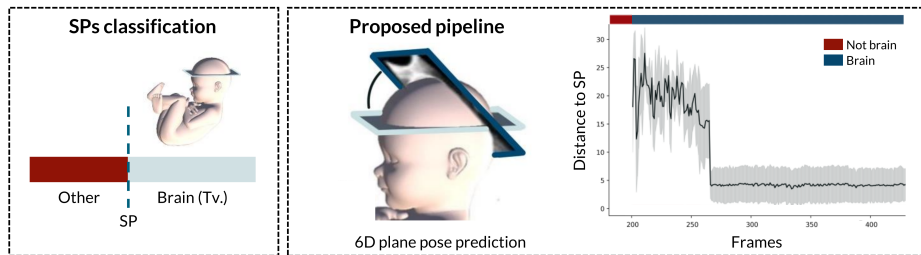


Fig. 1: Comparison of the proposed approach with SPs classification approaches.

notate the canonical pose of TV SP on training 3D US volumes and use them to estimate relative proximity to these planes at inference time; 4) We validate our pipeline on recorded video of real fetal scans from sonographers with varying expertise and demonstrate that our plane proximity predictions indicate a tendency for alignment with expert assessment of SP quality.

2 Methods

In this work, we focus on guidance toward the TV SP in the fetal brain. Our proposed pipeline involves 3 main steps: 1) detection and segmentation of the fetal brain on a US image; 2) plane pose regression on masked fetal brain images; 3) measurement of proximity to target SP. The method is trained in a semi-supervised manner using a combination of labeled images of SP together with unlabeled images from 3D US volumes.

2.1 Semi-supervised fetal brain segmentation

Our segmentation and classification model (Figure 2) is based on U-Net [18]. The encoder, ‘timm-efficientnet-b0’ [19] pre-trained on ImageNet [20], takes as input an image with dimensions $C \times H \times W$, where $C=3$ is the number of channels, $H=320$ is the height, and $W=320$ is the width. The model has two decoder heads. The segmentation head is a conventional U-Net decoder with skip connections; the classification head contains a Global Average Pooling, a Fully Connected Layer, and a sigmoid activation for binary classification (“brain”, “not-brain”).

The model is trained with 3 losses. The classification head is trained with Binary Cross Entropy ($\mathcal{L}_{classification}$). The segmentation head is trained on labeled data with an average of Dice and Binary Cross Entropy ($\mathcal{L}_{Seg, labeled} = (\mathcal{L}_{Dice}(M'_L, M) + \mathcal{L}_{BCE}(M'_L, M))/2$). The segmentation head is also trained on unlabeled volume slices with $\mathcal{L}_{Seg, unlabeled}$, calculated as the mean square error (MSE) between the segmentations of images acquired at the same pose from the different volumes: $\mathcal{L}_{Seg, unlabeled} = \frac{2}{n(n-1)} (\sum_{i=1}^{n-1} \sum_{j=i+1}^n \|M'_{U,i} - M'_{U,j}\|_2)$, where n is the number of volumes in the training and validation sets ($n = 3$ and

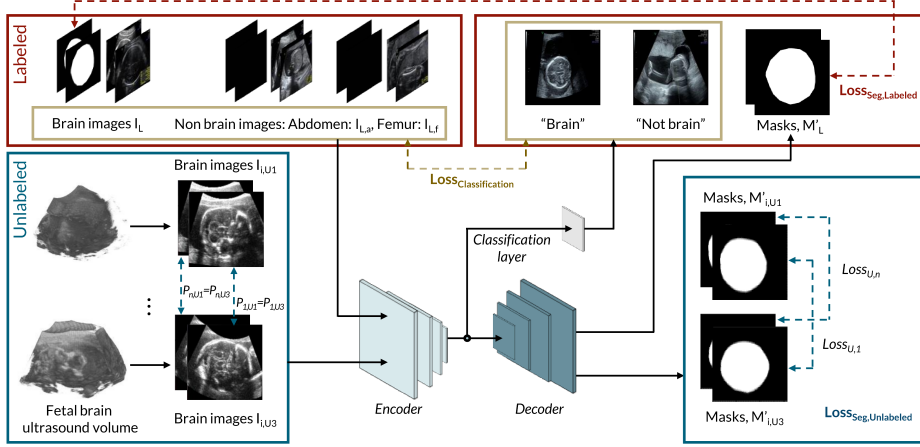


Fig. 2: Components of our semi-supervised learning model. Labeled (brain and non-brain) and unlabeled brain US images are fed into a UNet. The encoder extracts the features from the images; the classification branch takes the encoder output and classifies the images as containing brain or not, whereas the decoder predicts the masks for both labeled and unlabeled brain images.

$n = 2$, respectively), $M'_{U,i}$ and $M'_{U,j}$ are the predicted masks for the unlabeled images. The total loss is then:

$$\mathcal{L}_{Total,SS-Seg+Class} = \mathcal{L}_{Seg,labeled} + \alpha \mathcal{L}_{Seg,unlabeled} + \mathcal{L}_{classification} \quad (1)$$

where $\alpha = 0.5$ is a balancing coefficient that controls the relative weight of the loss for unlabeled versus labeled images.

2.2 Plane pose regression

We use an 18-layer residual convolutional neural network (CNN) (ResNet-18) [21] as a backbone for feature extraction with the pre-trained ImageNet weights. We modified the network by re-initializing the fully connected layer based on the representation's dimension (nine parameters) and adding a regression head to output the rotation and translation representations directly. The network receives a masked US image I (128×128) obtained by slicing the volume and applying the mask generated by the SS-Seg+Class network, and its 6D pose with respect to the center of the fetal brain US volume $\theta_{GT} = (t_x, t_y, t_z, \alpha_x, \alpha_y, \alpha_z)$. We use this information as the ground truth label for network training and validation. The CNN learns to predict the 6D pose $\theta_{Pred} = (t'_x, t'_y, t'_z, \alpha'_x, \alpha'_y, \alpha'_z)$.

For both translation and rotation we used as loss the MSE between predicted $(\mathbf{t}', \mathbf{R}')$ and ground truth (\mathbf{t}, \mathbf{R}) values: $\mathcal{L}_{Translation} = \frac{1}{N} \sum_{t=1}^N \|\mathbf{t}' - \mathbf{t}\|_2$, $\mathcal{L}_{Rotation} = \frac{1}{N} \sum_{t=1}^N \|\mathbf{R}' - \mathbf{R}\|_2$ where N denotes the total number of images I within one training epoch, \mathbf{t}' denotes the predicted translation component and \mathbf{t}

the label. \mathbf{R} is the 3×3 rotation matrix obtained from the ground truth rotation vector $\mathbf{r} = (r_x, r_y, r_z)$ and \mathbf{R}' is the 3×3 rotation matrix obtained from the 6 parameters r_1, \dots, r_6 as the output of the networks. The total loss function is then computed as: $\mathcal{L}_{Total} = \mathcal{L}_{Rotation} + \lambda \mathcal{L}_{Translation}$. where λ is a balancing coefficient. To compute the proximity of the US video frame to a labeled TV SP during inference, we use euclidean distance for translation and the angle between the normal vectors of the frame (\vec{N}_f) and the SP (\vec{N}_{SP}) for rotation ($\alpha = \arccos\left(\frac{(\vec{N}_f \cdot \vec{N}_{SP})}{(\|\vec{N}_f\| \|\vec{N}_{SP}\|)}\right)$), explicitly excluding in-plane rotation components as they do not alter the plane appearance.

3 Experiments and Results

All our models are implemented in *PyTorch* and trained using a single Tesla[®] V100-DGXS-32GB GPU of an NVIDIA[®] DGX station.

Datasets We use 6 fetal brain US volumes from [22] (singleton pregnancy with no abnormal findings) acquired at the axial TV SP from 20-25 weeks gestational age (GA) pregnancies. The volumes are aligned in translation, rotation, and scale. All volumes were processed to be isotropic with a voxel size of $0.5 \times 0.5 \times 0.5$ mm and an average size of $249 \times 174 \times 155$ mm (*coronal* \times *axial* \times *sagittal*). We slice these volumes with random rotations and offsets from the volume center within a fixed range to avoid slices with poor overlap with the volume. We acquired 22029 images for each volume. We train the segmentation model using sets of slices acquired in the same pose for different registered volumes. The pose regression model is trained with slices paired with their ground truth pose. To estimate proximity to the target plane, an obstetrician annotated the pose of the TV SP using a 3D interface implemented in Unity.

In addition to volume slices, we use a US dataset of 346 US images acquired from 42 fetuses during the second trimester with labeled segmentation masks of the brain, abdomen, and femur initially used in the AutoFB work [7]. The dataset includes 135 brain images and 211 non-brain images (abdomen and femur).

Finally, we test our complete pipeline on routine second-trimester fetal US scans recorded at *anonymous hospital* using a Voluson[™] E8[®] US machine (GE Healthcare, Chicago, Illinois). The study was approved by *anonymous regulatory body*. The full videos used in our pipeline are available⁸.

Brain segmentation and classification The labeled images were split into 205 for training, 53 for validation, and 97 for testing, with a balanced distribution of “brain” and “not brain” classes in each set. Images are cropped and resized to 320×320 . On the other hand, the unlabeled volume slices are split into 6 folds (1 for each volume), and we train 6 different segmentation models in a leave-one-out manner with 3 training and 2 validation volumes (combining a fixed

⁸ *Link to videos

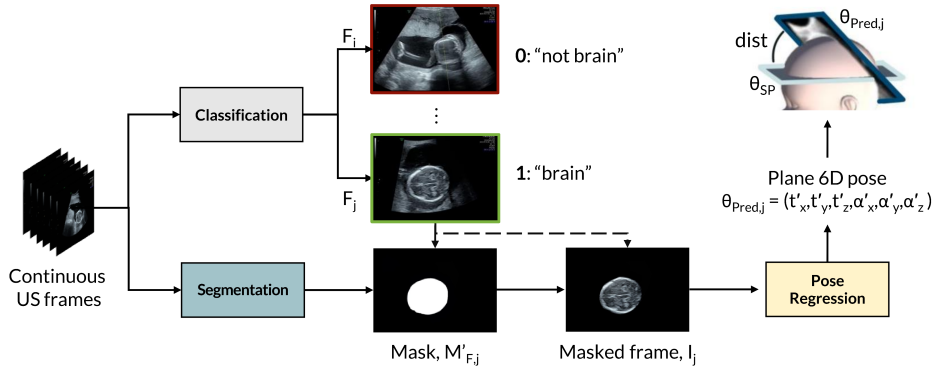


Fig. 3: Inference pipeline on frames from US videos. The frames are classified as containing or not the brain; if the brain is detected, the mask is generated, and the frame with the mask applied is fed into a pose regression network to regress the 6D pose of the frame and compute the distance to the SP.

labeled training set with leave-one-out unlabeled folds). We do this to enable evaluating the downstream pose regression model using Leave One Out Cross-Validation (LOOCV) without any data leakage.

Each segmentation model is trained in 3 stages. First, we train a model S-Seg in a fully supervised manner on the fixed labeled training set for 50 epochs with a learning rate $lr = 0.003$. Flipping, rotation, gaussian noise, elastic transform, brightness and contrast change augmentations are added. Then we add the unlabeled training set and obtain the model SS-Seg by training 150 more epochs, with $lr = 0.008$, using a StepLR scheduler with a step size of 50 epochs and a reduction rate $\gamma = 0.5$. Finally, the classification head is added, and we obtain a model SS-Seg+Class by further fine-tuning for 150 epochs with $lr = 0.00003$. We use a batch size of 8 during the entire process.

We compare our results against AutoFB [7], which performs 3-class segmentation of the femur, brain, and abdomen. It was trained in a fully supervised manner on the same labeled training set as our model for 600 epochs with early stopping (patience of 50 epochs). Table 1 reports the mean Intersection over Union (IoU) (mIoU) for the labeled test set. We also report mean IoU between pairs of slices at the same pose from the validation sets to measure segmentation consistency in arbitrary slices. For SS-Seg and SS-Seg+Class, we report the average performance of our 6 trained models, while for S-Seg and AutoFB, we only report one model trained on the fixed labeled training set.

Plane pose regression For both training and inference with our pose regression model, we start by taking brain segmentation predictions, dilating them with a 30×30 kernel, and masking out the irrelevant portions of the image. We train 6 pose regression models on masked images (one for each segmentation model) to perform LOOCV. We use 20% of the training data for validation.

Table 1: Mean Intersection over Union across images obtained for the experiments performed with the LOOCV for AutoFB [7], S-S, SS-S, and SS-S+Class.

mIoU	AutoFB [7]	S-Seg	SS-Seg	SS-Seg+Class
Test Labeled	0.9170	0.9537	0.9144	0.9482
Validation Unlabeled	0.7338	0.5660	0.7975	0.8278

Table 2: Average translation and rotation errors of our pose regression model with and without segmentation masking.

	trans_{median}	trans_{mean}	trans_{min}	trans_{max}	rot_{median}	rot_{mean}	rot_{min}	rot_{max}
No masks [*]	2.97	4.11	0.05	47.48	6.63	8.96	0.16	126.52
With masks	2.49	3.35	0.02	42.53	5.62	6.96	0.09	109.32

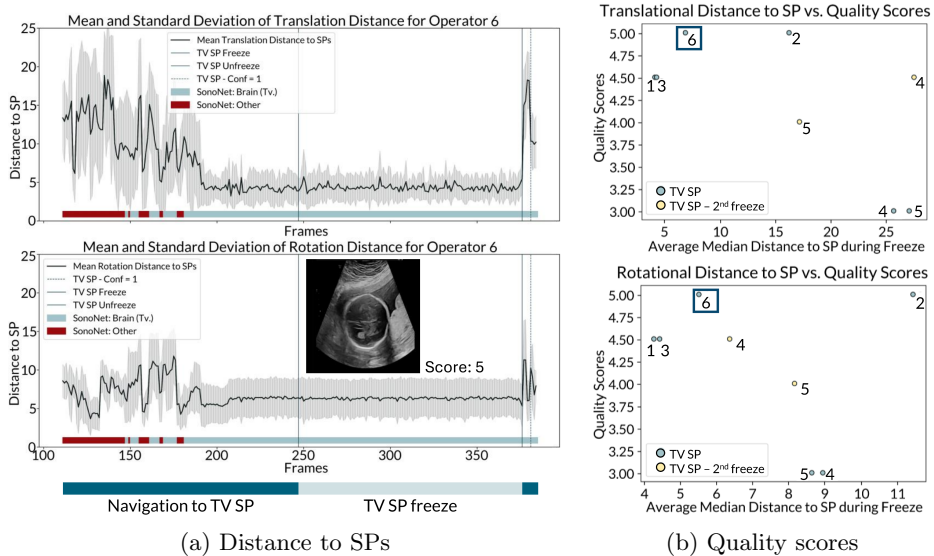


Fig. 4: (a) Distances to TV SP and SonoNet’s predictions. (b) Obstetrician assessment of the TV SP per operator, with SP re-acquisitions for operators 4 and 5 due to required structures not being visible and the plane being too oblique.

The network was trained for 200 epochs with a batch size of 64 using Adam optimizer, with a learning rate $lr = 0.0001$. We report the performance of our model with and without segmentation masking in Table 2.

Ultrasound video The SS-Seg+Class network was applied to the US videos described in Section 3. We extract frames from the US videos at a frame rate of 10 Hz to have a manageable number of frames for analysis, reducing computational

load while retaining sufficient temporal resolution to capture the relevant US imagery. Upon extraction, the frames were fed to the SS-Seg+Class network to detect the fetal brain and isolate the area of interest from the surrounding anatomical structures. The brain images identified and masked were then fed to the plane pose regression network for obtaining the 6D poses. For each frame, we compute the distance of the plane to the TV SP, previously annotated on the US volumes. The obstetrician was asked to score the frozen TV SP individually for quality control using the scoring system described by Salomon et al. [23]. The reviewer was blinded to whether the images being scored were from the novice or the expert groups. In parallel, we fed the entire video through a pre-trained SonoNet in its PyTorch implementation⁹ Figure 4 shows the translation and rotation distances to the TV SP, along with SonoNet’s predicted labels. Besides, critical moments in the video, such as when the sonographer freezes and unfreezes the image, are highlighted, along with the appearance of the frozen SP and the score assigned.

4 Discussion

Our SS-Seg+Class model shows robustness on both labeled and unlabeled data. Our model outperforms the others in segmenting SPs and non-SPs with improved mean IoU scores across images of 0.9482 on labeled images and 0.8272 on unlabeled images thanks to the inter-patient loss function (Table 1). The improved metrics with the use of masked images highlight the advancements in plane pose regression (Table 2). The adaptation of a model trained on static 3D US data to generalize to 2D US videos underscores the innovative potential of our approach. The predicted distances to the SP, along with SonoNet’s predicted labels, offer insights into the model’s precision in identifying and segmenting fetal brain structures (Figure 4a). The distance predictions indicate a tendency for alignment with the expert assessment of SP quality (Figure 4b). However, there are exceptions where the error in prediction arises from factors such as zooming (Op. 2) or in-plane translation, that is when the image is not well centered but still of good quality (Op. 4). These observations suggest that while the model shows potential in assisting sonographers to identify high-quality SPs with a degree of accuracy, these cases highlight areas for improvement. Notably, these findings are derived from a limited sample size, which underscores the need for further large-scale studies to establish the model’s effectiveness and reliability conclusively. Additionally, the model’s current training relies on a modest volume count, suggesting that expanding the training data with additional volumes or video data and integrating temporal models could further improve pose regression quality. Besides, the model could be applied to other brain SPs or other anatomical regions; nonetheless, extending generalized whole-fetus guidance may encounter obstacles due to fetal pose variability. Additionally, achieving real-time operation is critical for the practical application

⁹ <https://github.com/baumgach/SonoNet-weights>

of this model in clinical settings. The feasibility of real-time operation with the current architecture remains a question for further investigation.

Envisioning a future where sonographers receive information on the distance to SPs, we recognize the need for usability studies to assess whether more sophisticated navigation information can effectively aid operators in real-time.

5 Conclusion

This paper presents a novel approach to fetal US analysis, combining semi-supervised segmentation and classification of brain images with sensorless proximity detection to the TV SP. While traditional methods focus on SP identification, we emphasize the utility of recognizing the probe’s nearing SPs, facilitating earlier and more precise adjustments during scanning. Future work will target increased robustness to zoom variations and off-center anatomies typical in scans, as well as improving detection in cases of abnormal fetal development.

References

1. Hadlock, F.P., Harrist, R.B., Sharman, R.S., Deter, R.L., Park, S.K.: Estimation of fetal weight with the use of head, body, and femur measurements: A prospective study. *American Journal of Obstetrics and Gynecology* 151(3), 333–337 (1985)
2. Sarris, I., Ioannou, C., Dighe, M., Mitidieri, A., Oberto, M., Qingqing, W., Shah, J., Sohoni, S., Al Zidjali, W., Hoch, L., Altman, D.G., Papageorghiou, A.T.: Standardization of fetal ultrasound biometry measurements: Improving the quality and consistency of measurements. *Ultrasound in Obstetrics and Gynecology* 38(6), 681–687 (2011)
3. Bahner, D.P., Blickendorf, J.M., Bockbrader, M., Adkins, E., Vira, A., Boulger, C., Panchal, A.R.: Language of Transducer Manipulation: Codifying Terms for Effective Teaching. *Journal of Ultrasound in Medicine* 35(1), 183–188 (2016)
4. Sharma, H., Drukker, L., Chatelain, P., Droste, R., Papageorghiou, A.T., Noble, J.A.: Knowledge representation and learning of operator clinical workflow from full-length routine fetal ultrasound scan videos. *Medical Image Analysis* 69 (2021)
5. Salomon, L.J., Alfirevic, Z., Da Silva Costa, F., Deter, R.L., Figueras, F., Ghi, T., Glanc, P., Khalil, A., Lee, W., Napolitano, R., Papageorghiou, A., Sotiradis, A., Stirnemann, J., Toi, A., Yeo, G.: ISUOG Practice Guidelines: ultrasound assessment of fetal biometry and growth. *Ultrasound in Obstetrics and Gynecology* 53(6) (2019)
6. Baumgartner, C.F., Kamnitsas, K., Matthew, J., Fletcher, T.P., Smith, S., Koch, L.M., Kainz, B., Rueckert, D.: SonoNet: Real-Time Detection and Localisation of Fetal Standard Scan Planes in Freehand Ultrasound. *IEEE Transactions on Medical Imaging* 36(11), 2204–2215 (2017)
7. Bano, S., Dromey, B., Vasconcelos, F., Napolitano, R., David, A.L., Peebles, D.M., Stoyanov, D.: AutoFB: Automating Fetal Biometry Estimation from Standard Ultrasound Planes. *Lecture Notes in Computer Science (including subseries Lecture Notes in Artificial Intelligence and Lecture Notes in Bioinformatics)* 12907 LNCS, 228–238 (2021)

8. Avisdris, N., Joskowicz, L., Dromey, B., David, A.L., Peebles, D.M., Stoyanov, D., Ben Bashat, D., Bano, S.: Biometrynet: Landmark-based fetal biometry estimation from standard ultrasound planes. In: International Conference on Medical Image Computing and Computer-Assisted Intervention. pp. 279–289. Springer (2022)
9. Gao, Y., Beriwal, S., Craik, R., Papageorghiou, A.T., Noble, J.A.: Label Efficient Localization of Fetal Brain Biometry Planes in Ultrasound Through Metric Learning. Lecture Notes in Computer Science (including subseries Lecture Notes in Artificial Intelligence and Lecture Notes in Bioinformatics) 12437 LNCS, 126–135 (2020)
10. Rahmatullah, B., Papageorghiou, A., Noble, J.A.: Automated selection of standardized planes from ultrasound volume. In: Lecture Notes in Computer Science (including subseries Lecture Notes in Artificial Intelligence and Lecture Notes in Bioinformatics). pp. 35–42. Springer (2011)
11. Cuingnet, R., Somphone, O., Mory, B., Prevost, R., Yaqub, M., Napolitano, R., Papageorghiou, A., Roundhill, D., Noble, J., Ardon, R.: Where is my baby? a fast fetal head auto-alignment in 3d-ultrasound. In: 2013 IEEE 10th International Symposium on Biomedical Imaging. pp. 768–771 (2013)
12. Droste, R., Drukker, L., Papageorghiou, A.T., Noble, J.A.: Automatic Probe Movement Guidance for Freehand Obstetric Ultrasound. Lecture Notes in Computer Science (including subseries Lecture Notes in Artificial Intelligence and Lecture Notes in Bioinformatics) pp. 583–592 (2020)
13. Birlo, M., Edwards, P.J.E., Yoo, S., Dromey, B., Vasconcelos, F., Clarkson, M.J., Stoyanov, D.: CAL-Tutor: A HoloLens 2 Application for Training in Obstetric Sonography and User Motion Data Recording. *Journal of Imaging* 9(1), 6 (2022)
14. Di Vece, C., Dromey, B., Vasconcelos, F., David, A.L., Peebles, D., Stoyanov, D.: Deep learning-based plane pose regression in obstetric ultrasound. *International Journal of Computer Assisted Radiology and Surgery* 17(5), 833–839 (2022)
15. Di Vece, C., Le Lous, M., Dromey, B., Vasconcelos, F., David, A.L., Peebles, D., Stoyanov, D.: Ultrasound plane pose regression: assessing generalized pose coordinates in the fetal brain. *IEEE Transactions on Medical Robotics and Bionics* (2023)
16. Yeung, P.H., Aliasi, M., Papageorghiou, A.T., Haak, M., Xie, W., Namburete, A.I.: Learning to map 2D ultrasound images into 3D space with minimal human annotation. *Medical Image Analysis* 70 (2021)
17. Yeung, P.H., Aliasi, M., Haak, M., Xie, W., Namburete, A.I.L.: Adaptive 3D Localization of 2D Freehand Ultrasound Brain Images. In: LNCS. vol. 13434, pp. 207–217. Springer, Cham (2022)
18. Ronneberger, O., Fischer, P., Brox, T.: U-net: Convolutional networks for biomedical image segmentation. Lecture Notes in Computer Science (including subseries Lecture Notes in Artificial Intelligence and Lecture Notes in Bioinformatics) 9351, 234–241 (2015)
19. Tan, M., Le, Q.V.: EfficientNet: Rethinking Model Scaling for Convolutional Neural Networks
20. Deng, J., Dong, W., Socher, R., Li, L.J., Kai Li, Li Fei-Fei: ImageNet: A large-scale hierarchical image database pp. 248–255 (3 2010)
21. He, K., Zhang, X., Ren, S., Sun, J.: Deep residual learning for image recognition. In: Proceedings of the IEEE Computer Society Conference on Computer Vision and Pattern Recognition. pp. 770–778 (2016)
22. Pistorius, L.R., Stoutenbeek, P., Groenendaal, F., De Vries, L., Manten, G., Mulder, E., Visser, G.: Grade and symmetry of normal fetal cortical development: A

- longitudinal two- and three-dimensional ultrasound study. *Ultrasound in Obstetrics and Gynecology* 36(6), 700–708 (2010)
23. Salomon, L., Winer, N., Bernard, J., Ville, Y.: A score-based method for quality control of fetal images at routine second-trimester ultrasound examination. *Prenatal Diagnosis: Published in Affiliation With the International Society for Prenatal Diagnosis* 28(9), 822–827 (2008)